

# Interweaving Anion Templatation

MICHAEL D. LANKSHEAR AND PAUL D. BEER\*

*Inorganic Chemistry Laboratory, Department of Chemistry,  
University of Oxford, South Parks Road, Oxford OX1 3QR,  
United Kingdom*

Received January 30, 2007

## ABSTRACT

A new general interweaving anion templatation strategy for the formation of interpenetrated and interlocked architectures is presented. Furthermore, the functional properties of the resulting systems, which have novel anion binding and sensory properties, are discussed.

## Introduction

The threading and interlocking of two or more components has been of interest to mankind since time immemorial. At the macroscopic level, such threading may be encountered in everyday life, from sewing to chain-link fences, in high art, and in mechanical devices. More recently, the intense interest in the production of nanotechnological devices has led to a strong motivation to develop such interpenetrated motifs on the molecular scale; such “molecular machines” could potentially revolutionize modern society.<sup>1</sup> The basic motifs of these devices are illustrated in Figure 1. Thus, the threading of one component through another in a reversible manner leads to a pseudorotaxane, and where this threading is irreversible (being blocked by suitable stopper units), a rotaxane is formed. The permanent interlocking of two ring components leads to a catenane.

Manufacturing such elegant architectures on the molecular scale is not, unfortunately, a trivial matter as it is obviously not possible to manually thread the components. The earliest syntheses of interpenetrated and

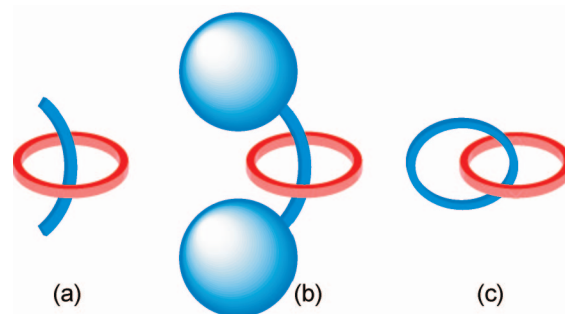


**FIGURE 1.** Elementary interpenetrated and interlocked motifs: (a) [2]pseudorotaxane, (b) [2]rotaxane, and (c) [2]catenane. The number in square brackets corresponds to the number of interpenetrated components (2 for all these systems).

interlocked compounds thus relied on the statistical association of two components, which resulted in low yield and laborious procedures.<sup>2,3</sup> Over the past 25 years, however, the application of designed self-assembly approaches has led to the elaboration of a panoply of fascinating motifs based on mutual interpenetration.<sup>4</sup> Two key types of self-assembly have been employed (Figure 2). In the first, the assembly is mediated by direct interaction between the building blocks in the reversible formation of a precursor complex, which is then “trapped” to give a permanently interlocked system; the example shown illustrates the penetration of a dibenzo-24-crown-8 ring by a dibenzylammonium-based thread, which occurs through a combination of electrostatic and hydrogen bonding interactions.<sup>5</sup> Subsequent “stoppering” then yields a [2]rotaxane. Alternatively, an interweaving template<sup>6</sup> may be used to direct complex formation. In this case, the template may be removed from the interlocked system following synthesis, which is advantageous as it should distinguish the properties of the resulting species from the method used to form it. The archetypal example of such a template is provided by the seminal work of Sauvage and co-workers, who have used the tetrahedral directing nature of Cu(I) metal cations to control the formation of a wide range of interlocked species, including the [2]catenane that is illustrated.<sup>7</sup>

The interweaving templates used historically have invariably been cationic. This is a natural consequence of the strong coordinative geometric preference of transition metals, which allows the accurate orientation of the two interweaving components. As anions do not benefit from such strong geometric preferences, and their coordination chemistry remains substantially less well elucidated,<sup>8</sup> it is perhaps unsurprising that they have received considerably less attention as potential templates, in spite of the potential for interesting function in the resulting materials.<sup>9</sup> Thus, although interpenetration has been accomplished using anion-dependent self-assembly processes, such as those based on organic phenoxides<sup>10,11</sup> or hexafluorophosphate anions,<sup>12</sup> the anion always forms a part of the product; no designed approach for exploiting

Michael Lankshear was born and raised in Dorchester, Dorset, and gained a first class honors degree in chemistry from the University of Oxford in 2003. He conducted his final year undergraduate research project under the auspices of Professor Paul Beer and remained in the same group to study for his D.Phil. In his time at Oxford, Michael has been awarded scholarships of Keble College (2000) and Trinity College (2004) and was recognized for the quality of his undergraduate thesis (2003).

Paul Beer gained a first class honors degree in chemistry from King's College London in 1979, and he also studied there for his Ph.D. under the supervision of Dr. C. Dennis Hall. A Royal Society European postdoctoral fellowship then allowed him to work with Professor Jean-Marie Lehn at the Université Louis Pasteur (Strasbourg, France), after which in 1983 he obtained a demonstratorship at the University of Exeter. A year later he moved to the University of Birmingham to take up a New Blood Lectureship, winning the Royal Society of Chemistry (RSC) Meldola Medal in 1987. In 1990, he moved to a lectureship at the Inorganic Chemistry Laboratory, University of Oxford, where he is also a tutorial fellow at Wadham College. He has subsequently been awarded the international UNESCO Javed Husain Prize (1993), the RSC Corday-Morgan Medal (1994), a university professorship (1998), and the RSC Tilden Medal and Lectureship (2004). Professor Beer's research interests cover many areas of supramolecular and coordination chemistry, including the construction of redox- and photo-active host systems for electrochemical and optical sensing of target cationic and anionic guest species, ion pair recognition, anion templatation, and transition metal-directed assembly of polymetallic molecular architectures.

\* Corresponding author. E-mail: paul.beer@chem.ox.ac.uk.

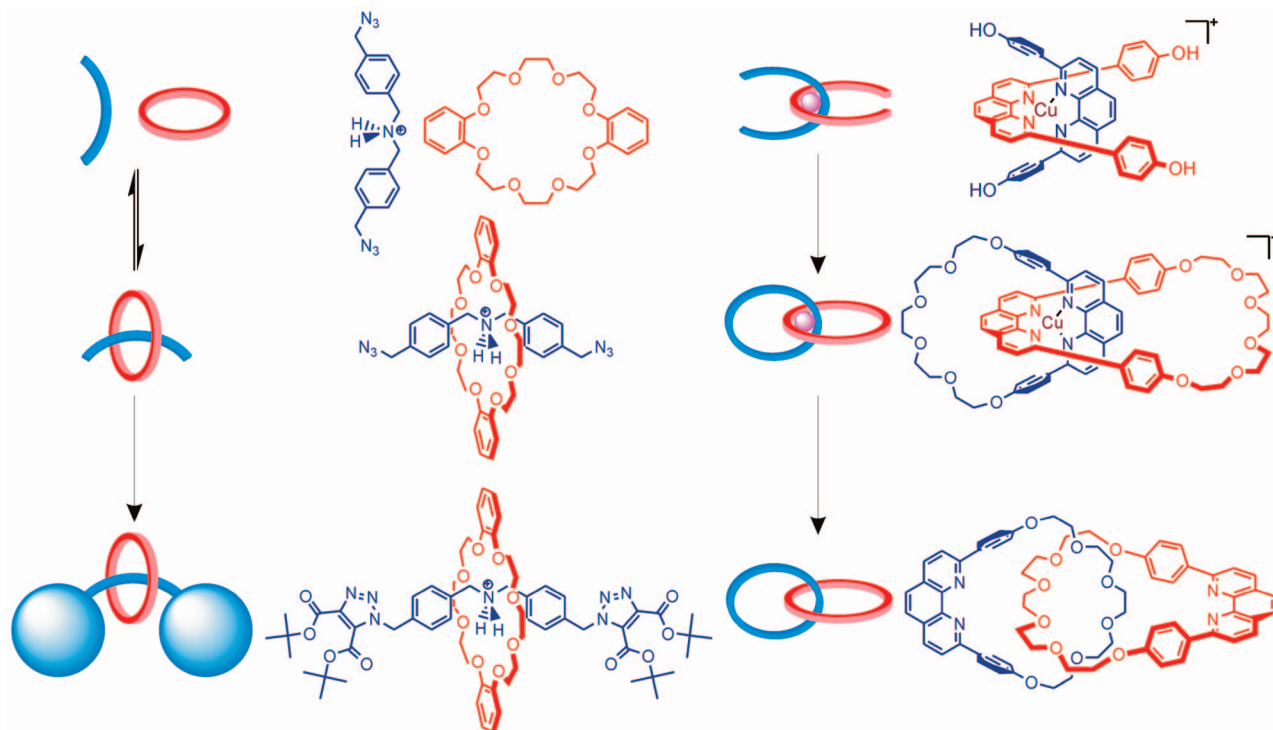


**FIGURE 2.** Two methods of generating interlocked architectures. Self-assembly of a thread and ring component (left) followed by stopping yields a [2]rotaxane, while the template-directed assembly of two orthogonal components (right) followed by clipping yields a [2]catenane, with template removal possible in this case.

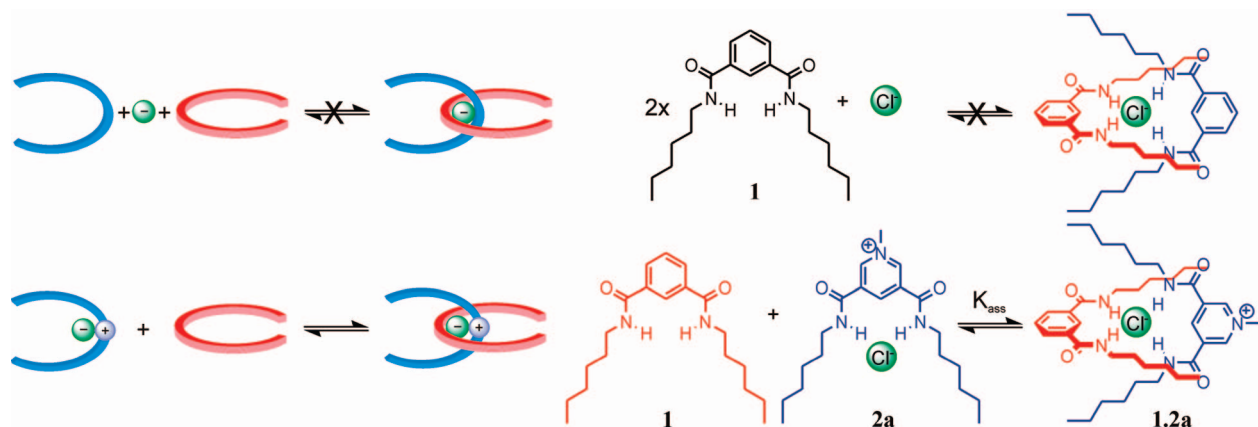


**FIGURE 3.** Anion-templated assembly of orthogonal complexes. In acetone- $d_6$ , the  $K_{\text{ass}}$  value was  $100 \text{ M}^{-1}$ .

discrete anion templates has been documented. With an eye to addressing this deficiency, and using the resulting systems as novel sensory and device-like materials, we present within this Account such a strategy based on interweaving anion templatation.

### Design of a General Anion Templatation Motif

A fundamental requirement for an interweaving template is the ability to direct two components in an orthogonal manner. While such a feat has been accomplished using cations, using anions for this purpose required careful consideration of design (Figure 3). First, appropriate anion coordination units had to be selected; as receptors such as **1** based on the isophthalamide binding cleft had previously been shown to bind halide anions strongly in

nonpolar organic solvents through convergent hydrogen bonding,<sup>13</sup> these were chosen.<sup>14</sup> Unfortunately, the binding stoichiometry of this motif with halides was 1:1 in all solvents studied, making it impossible to form orthogonal complexes on the basis of this alone. However, utilization of a tightly associated pyridinium–chloride ion pair (**2a**) as one of the assembling components rectified this problem. In acetone- $d_6$ , the pyridinium cation and chloride anion associate strongly in a 1:1 manner, but importantly, the chloride anion presents a vacant coordination meridian to which a molecule of **1** can bind. The resulting orthogonal complex **1.2a**, with a pseudotetrahedral geometry enforced by steric interactions, was demonstrated to form by  $^1\text{H}$  NMR methods in acetone- $d_6$  with an association constant of  $100 \text{ M}^{-1}$ .

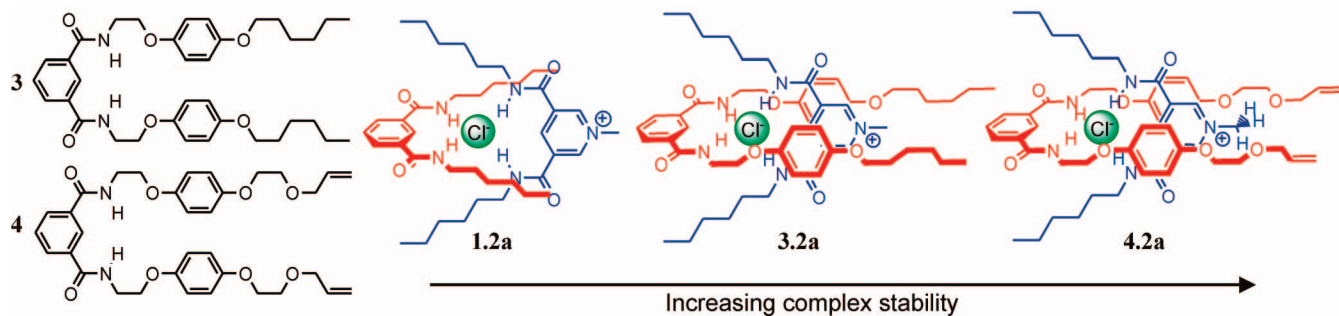


**FIGURE 4.** Increasing the strength of orthogonal complex formation using secondary interactions.

Augmentation of the primary anion-mediated association of the two components could be accomplished through alterations in the structure of the neutral component (Figure 4).<sup>15</sup> Thus, sequential introduction of hydroquinol diether (3) and extra ether oxygens (4) led to incremental enhancements in the anion-templated orthogonal complex association constants, as measured by <sup>1</sup>H NMR methods in dichloromethane-*d*<sub>2</sub>. The hydroquinol diether functionality allows  $\pi$ -stacking/charge transfer interactions to occur with the pyridinium cation unit, with such an interaction being detected by UV-visible spectroscopy. The extra ether oxygens then act as hydrogen bond acceptors for the weakly acidic protons of the *N*-methyl group. These interactions are secondary to the anion templation event, as no orthogonal complex formation could be detected in the presence of noncoordinating anions, such as hexafluorophosphate. In light of the strength of the primary anion recognition event in concert with these secondary interactions, it was postulated that a robust motif for the anion-mediated interpenetration of two components had been elucidated.

### Anion-Mediated Interpenetration

Replacement of the neutral acyclic component of the assemblies described above with a suitable macrocycle should therefore lead to interpenetrated complexes, [2]pseudorotaxanes. Indeed, such an assembly proved to be possible using the macrocycle **5** and thread **2a** (Figure 5).<sup>14</sup> This could readily be proved through consideration of the differences between the <sup>1</sup>H NMR spectra of the free components and the 1:1 mixture in acetone-*d*<sub>6</sub>; foremost, it is evident that significant shifts in the protons involved in anion complexation are observed. Thus, upfield shifts in the pyridinium aromatic and amide protons (A) and downfield shifts in the macrocycle isophthalyl and amide protons (C) are seen, these being consistent with competitive coordination of chloride. Secondary hydrogen bonding interactions may be evidenced by a downfield shift in the pyridinium *N*-methyl proton signal (B), and a charge transfer/ $\pi$ -stacking interaction by an upfield shift in the macrocycle hydroquinol diether proton signal (D). Additionally, as in the formation of orthogonal complexes **3.2a** and **4.2a**, this charge transfer interaction between the hydroquinol diether rings of the macrocycle and the pyridinium unit of the thread could be detected through UV-visible spectroscopic means in acetone. The strength of this pseudorotaxane assembly is critically dependent

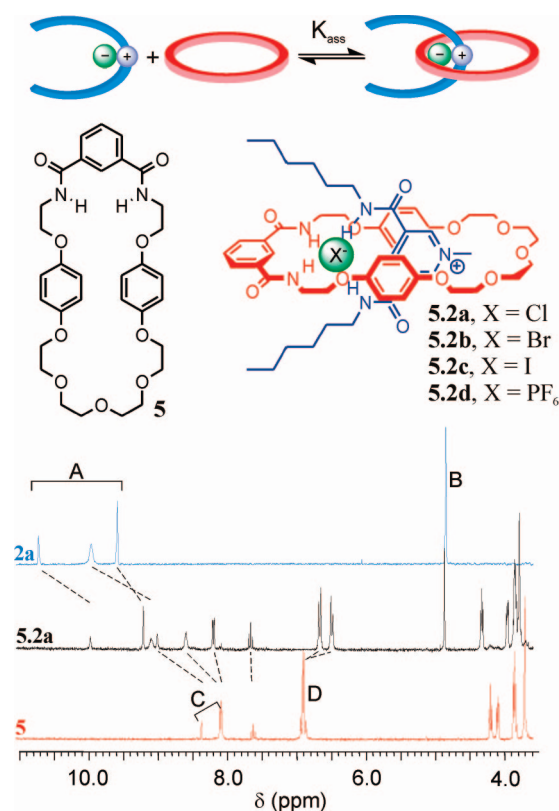


**FIGURE 5.** Formation of anion-templated [2]pseudorotaxane. General scheme (top), macrocycle **5** and pseudorotaxane **5.2a** (middle), and <sup>1</sup>H NMR spectroscopic evidence of pseudorotaxane formation (bottom). For spectrum labeling, see the text.

on the nature of the templating anion. Thus, when the thread counterion is chloride (**2a**), the pseudorotaxane has an association constant of 2400 M<sup>-1</sup>, but for bromide (**2b**), iodide (**2c**), and hexafluorophosphate (**2d**), the constants are lower, being 700, 65, and 35 M<sup>-1</sup>, respectively. This reflects the relative complexation abilities of these anions.

The strength of pseudorotaxane assembly was furthermore found to depend on the size of the macrocyclic unit (Figure 6).<sup>16</sup> As macrocycle ring size was increased, the stability of the resulting pseudorotaxane decreased. Thus for macrocycles **6–8**, the pseudorotaxane association constants for **6.2a**, **7.2a**, and **8.2a** were 9500, 2400, and 950 M<sup>-1</sup>, respectively, in acetone-*d*<sub>6</sub>. Such variations in association constants could be ascribed to the entropic deficit of pseudorotaxane formation increasing with macrocycle size. There is also a significant favorable enthalpic contribution to the threading process; single-crystal X-ray

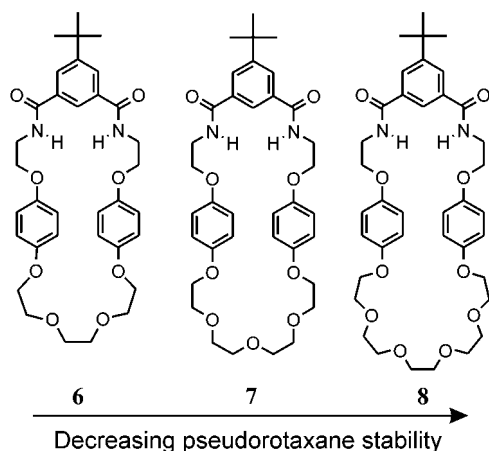


**FIGURE 6.** Variation of [2]pseudorotaxane stability with macrocycle ring size.

structures of **5.2a**, **6.2a**, and **8.2a** reveal that an optimum complementarity exists between the midsize macrocycle **5** (analogous to **7**) and the pyridinium thread, maximizing the secondary stabilizing interactions (Figure 7). These crystal structures also highlight the interpenetrated natures of the complexes, the coordination of the templating anion by both components, and the presence of the expected secondary charge transfer and hydrogen bonding interactions.

This anion-templated assembly is tolerant of other changes in the macrocycle structure. For example, the crown ether portion of **5–8** may be replaced with a calix[4]arene unit, as in **9** (Figure 8).<sup>17</sup> This macrocycle also undergoes [2]pseudorotaxane formation on treatment with thread **2a**, although the association constant is much reduced ( $170 \text{ M}^{-1}$  in acetone- $d_6$ ) compared to those of the simpler systems, possibly due to steric constraints. It is possible to enhance pseudorotaxane stability by improving the anion binding properties of the macrocycle. Thus, introduction of a 5-nitroisophthalamide function as in **10**, which increases the acidity of the amide hydrogen bond donors, also increases the observed pseudorotaxane association constant ( $240 \text{ M}^{-1}$  in acetone- $d_6$ ).

In addition to this tolerance of a range of macrocycle structures, the assembly process also supports a number of different thread species (Figure 9).<sup>16,18</sup> For example, threads based on the pyridinium nicotinamide unit (**11**) penetrate macrocycles **6–8** readily, with the same dependences on templating anion and macrocycle ring size that were seen for pyridinium thread **2**. However, the stabilities of these pyridinium nicotinamide-based pseudorotaxanes

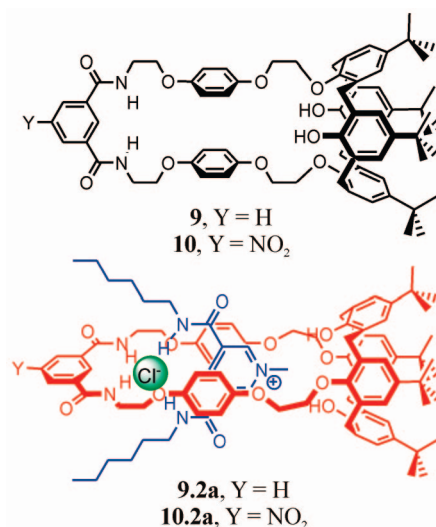


**FIGURE 8.** Calix[4]arene macrocycles for [2]pseudorotaxane formation.

are lower than those of their pyridinium analogues, with, for example,  $K_{\text{ass}}$  for **8.11a** being  $320 \text{ M}^{-1}$  compared to a value of  $980 \text{ M}^{-1}$  for **8.2a** (in acetone- $d_6$ ). This reduction is due to the absence of secondary hydrogen bonding interactions stabilizing the pseudorotaxane complex, which can clearly be observed in the single-crystal X-ray structure of **7.11a**. Furthermore, pseudorotaxane assemblies based on imidazolium (**12**), benzimidazolium (**13**), and guanidinium (**14**) thread motifs were also demonstrated. For these thread systems, however, analysis of the pseudorotaxane formation event was complicated by weak ion pairing. For the pyridinium and nicotinamide thread systems **2** and **11**, the thread–anion ion pairing was found to be very strong, and thus, essentially the macrocycle bound the anion and thread as a single unit; however, in the more weakly ion paired systems (**12d** binds chloride with an association constant of  $1800 \text{ M}^{-1}$  in acetone- $d_6$ ), this assumption was not valid, as significant quantities of “free” anion and thread were present. The two potential competing equilibria that may be observed are shown in Figure 9. Of these,  $K_{\text{th}}$ , which corresponds to the threading of the cationic portion of the thread alone, is known to be negligible. However, the contribution of the macrocycle sequestering the anion ( $K_{\text{seq}}$ ) could not be ignored; we had to account for this in measuring the pseudorotaxane formation constants for threads **12–14**. The magnitudes of corrected  $K_{\text{ass}}$  values for these systems were lower than those found for **2** or **11**, with, for example,  $K_{\text{ass}}$  for **6.13a** being  $320 \text{ M}^{-1}$  in acetone- $d_6$ . This is a consequence of

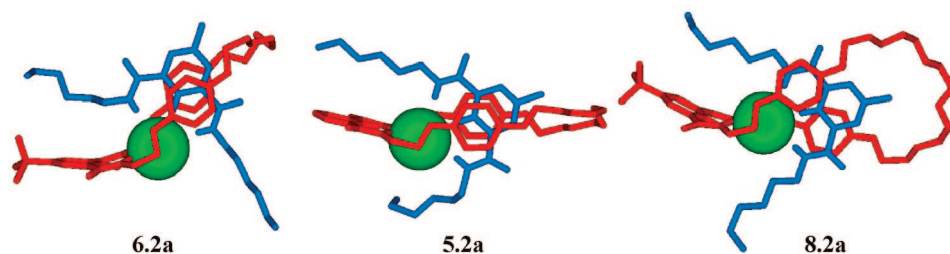


**FIGURE 7.** Single-crystal X-ray structures of [2]pseudorotaxanes **6.2a**, **5.2a**, and **8.2a**. All hydrogens except those in the primary anion coordination sphere have been omitted for clarity. Chloride is represented as a space-filling sphere.

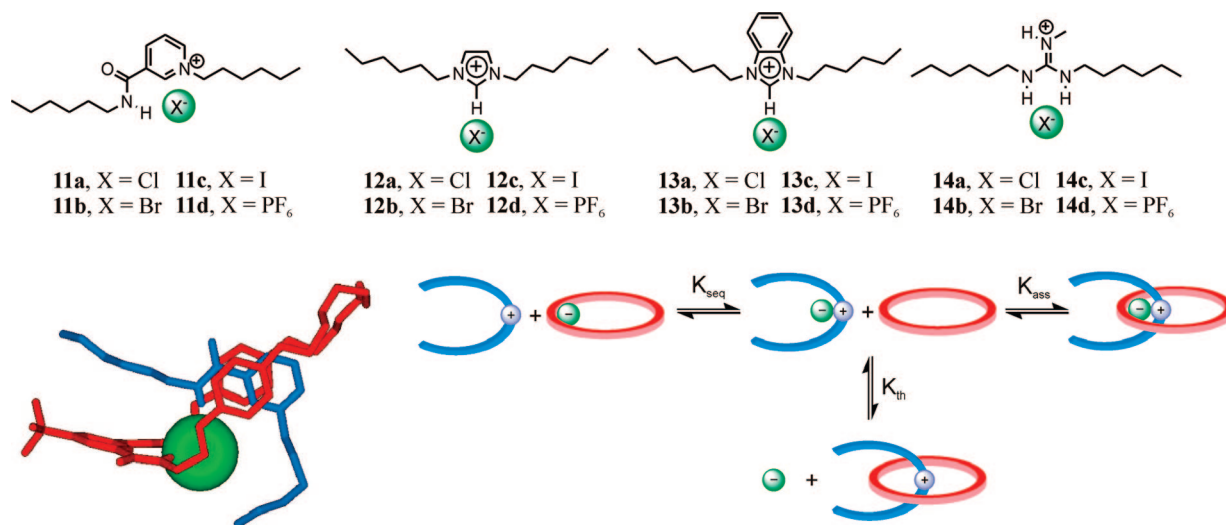


**FIGURE 9.** Alternative threads for pseudorotaxane assembly. Chemical structures (top), single-crystal X-ray structure of **7.11a** (bottom left), and a summary of potential solution equilibria present on threading (bottom right).

both weaker ion pairing and weakened secondary interactions. For thread **14**, it was not possible to obtain association constant data, although evidence for pseudorotaxane formation could be inferred through ROESY NMR spectroscopic experiments.

This general anion templation methodology may therefore be used to mediate the interpenetration of a variety of different threads and macrocycles. The stabilities of the resulting pseudorotaxane systems are heavily dependent on the nature of the components, in particular the nature of the templating ion, but also the size of the macrocycle, propensities for secondary stabilizing interactions, and the strength of thread–anion pairing. The successful interpenetration of such a variety of systems using anion templation suggested that this assembly process was appropriate for the formation of permanently interlocked derivatives.

## Routes to Permanently Interlocked Structures

To access anion-templated interlocked structures, a suitable method of trapping assemblies such as those outlined above needed to be identified. The primary method chosen for this purpose was olefin ring closing metathesis, mediated by Grubbs' catalyst,<sup>19</sup> which had been previously used to “clip” other precursors to form catenanes<sup>20,21</sup> and rotaxanes.<sup>22</sup> Grubbs' catalyst was deemed particularly suitable in this case as the mechanism of catalysis did not include any intermediates which would interfere with the anion templation event.

The scope of this ring closing metathesis approach was tested by the clipping of acyclic precursors such as **4** and **15** (Figure 10).<sup>23</sup> The lowest-energy conformation of this isophthalamide motif has been determined to be *syn-anti*,<sup>13</sup> which results in the divergent orientation of the precursor arms. Consequently, on treatment with Grubbs' first-generation catalyst in dichloromethane, neither of the cyclic products (**16** or **17**) was obtained. A chloride anion template orients these allylic arms prior to reaction, allowing the formation of the macrocycles, with the *trans*-

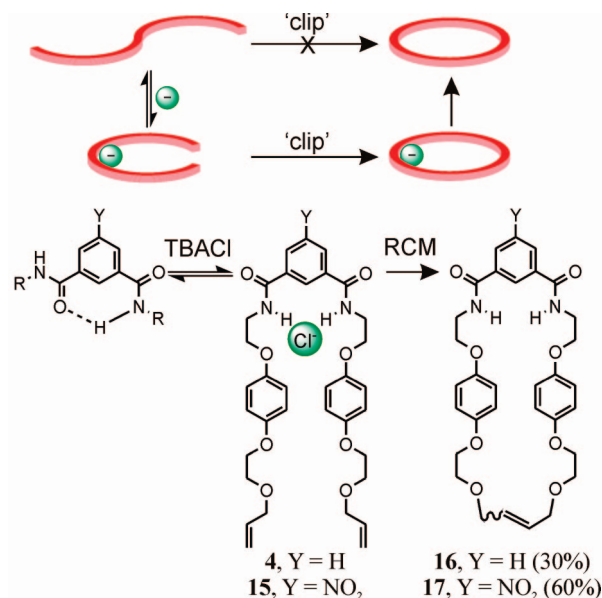


**FIGURE 10.** Anion-templated macrocycle formation using ring closing metathesis.

isomeric forms dominating. A higher yield of **17** was achieved, which is a result of the precursor having a greater affinity for the anion template.

The application of such an anion-templated ring closing reaction to an orthogonal complex will produce a [2]rotaxane when one component is terminated by bulky stopper units (Figure 11).<sup>15</sup> Thus, when complex **4.18a**, assembled in dichloromethane, was treated with Grubbs' first-generation catalyst, [2]rotaxane species **19a** was formed in 47% yield. Use of chloride-based thread **18a** gave an optimal yield of **19**; use of the bromide, iodide, and hexafluorophosphate salts **18b–d** did not give any [2]rotaxane product. The interlocked nature of **18a** could be inferred both from NMR spectroscopy and from single-crystal X-ray analysis (Figure 12). The latter clearly demonstrated the expected encirclement of chloride by the primary anion coordination spheres of the two components, as well as the expected secondary stabilizing

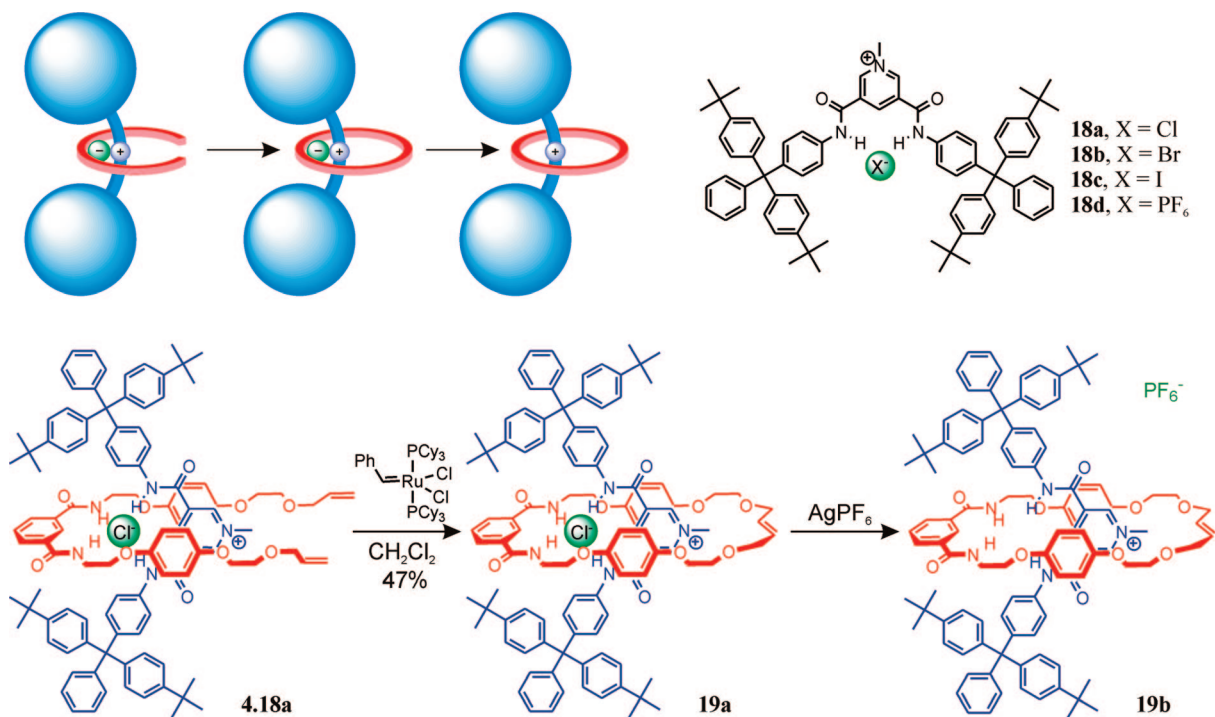


**FIGURE 11.** Formation of [2]rotaxanes. General scheme (top left), stoppered thread (top right), and formation of rotaxanes **19a** and **19b** (bottom).

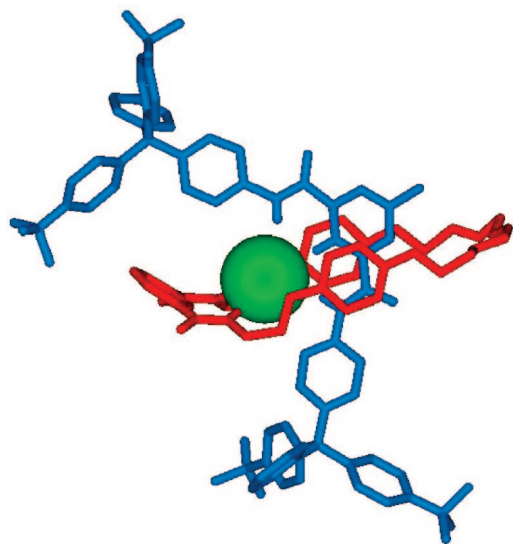


**FIGURE 12.** Single-crystal X-ray structure of **19a**. All hydrogens except those in the primary anion coordination sphere have been omitted for clarity. Chloride is represented as a space-filling sphere.

interactions. This interlocked rotaxane structure persisted following removal of the chloride anion template to give the hexafluorophosphate rotaxane **19b**. As mentioned in the Introduction, this is a crucial advantage of an interweaving template strategy. In this case, it leaves a unique three-dimensional anion-binding domain, the properties of which are discussed in the next section.

This synthetic route to [2]rotaxanes is tolerant of changes in the macrocycle structure. It has therefore been used to generate a number of species similar to **19a** (Figure 13).<sup>23</sup> Again, the process is highly dependent on the nature of the templating anion and furthermore

demonstrates a correlation with the structure of the macrocycle. Yield is therefore optimized for the nitro-containing rotaxane **21a**, which is a result of the precursor orthogonal complex assembly being more stable as a result of increased amide acidity. The yield of naphthyl-containing [2]rotaxane **22a** was somewhat lower, due to an increase in macrocycle size and flexibility. Importantly, the interlocked nature of these systems could withstand the removal of the chloride anion template.

If the precursor to be clipped in this manner is not an orthogonal complex containing bulky stopper groups but a pseudorotaxane, the resulting species will be a catenane (Figure 14).<sup>24</sup> Thus, treatment of an assembly constituting macrocycle **5** and thread **23a**, which contained olefinic termini, with Grubbs' catalyst in dichloromethane gave the [2]catenane **24a**, in 45% yield. As for the case of the [2]rotaxanes described above, the synthesis was highly dependent on the nature of the templating anion, with no product being obtained for iodide or hexafluorophosphate, and a low yield (6%) for bromide. Once again, the interlocked nature of the product could be established both from NMR spectroscopic experiments and from single-crystal X-ray analyses (Figure 15). It was clear from this structure that chloride is essential in controlling the orientation of the two interpenetrated components and that the secondary  $\pi$ -stacking and hydrogen bonding interactions involving the pyridinium function are present. Finally, as in the case of the [2]rotaxanes described above, it was possible to remove the interweaving chloride template to leave a vacant hydrogen bond donating cavity.

Other derivatives may be prepared by such anion-templated catenations (Figure 16). Thus, an interesting side product of these processes was the [3]catenane **25**,

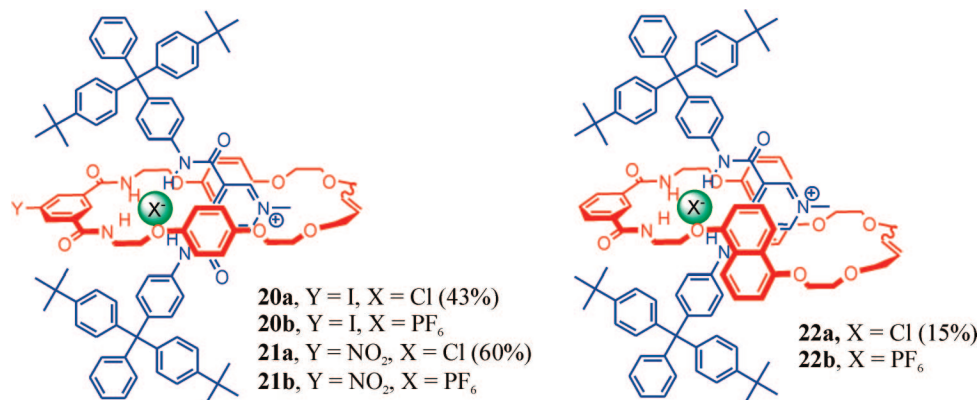


**FIGURE 13.** Anion-templated [2]rotaxanes. The percentages in parentheses correspond to the yields of the [2]rotaxane formation step from the acyclic precursors.

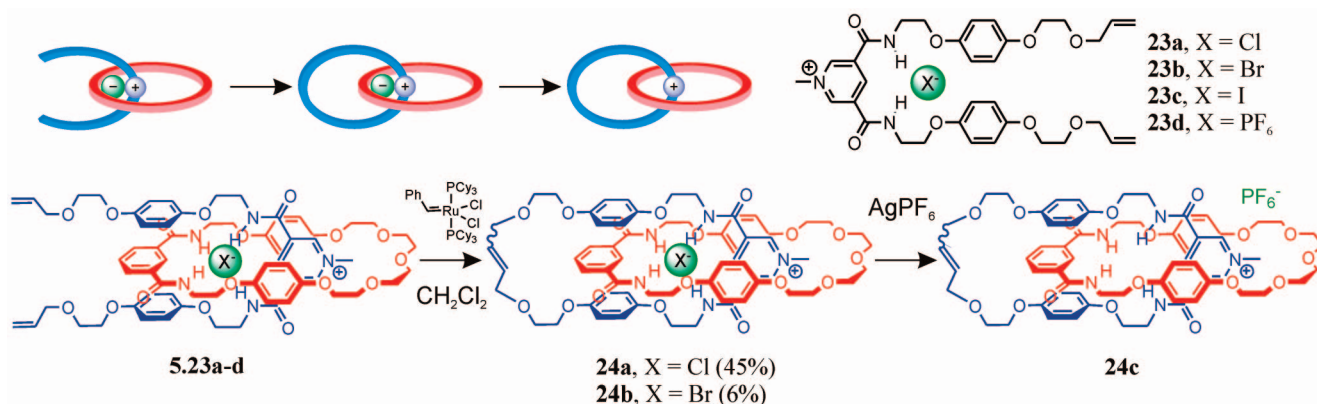


**FIGURE 14.** Formation of anion-templated catenanes from the [2]pseudorotaxane precursor. General scheme (top left), structure of thread precursor **23** (top right), and formation of catenane **24** (bottom). Yields for the catenane formation process are given in parentheses.

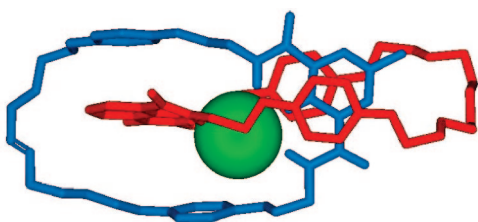


**FIGURE 15.** Single-crystal X-ray structure of **24a**. All hydrogens except those in the primary anion coordination sphere have been omitted for clarity. Chloride is represented as a space-filling sphere.

which formed in <5% yield during the synthesis of **24a**; interweaving anion templates may be used to generate interlocked structures of larger numbers of components. Furthermore, the assembly process is tolerant of changes in the neutral macrocyclic components, with, for example, the [2]catenane **26a** being formed in 29% yield from reaction of calix[4]arene macrocycle **9** and **23a**.<sup>17</sup> As before, this process was reliant on the presence of a suitable anion template, and exchange of this template to give the hexafluorophosphate salt **26b** also proved to be possible.

An alternative route to [2]catenanes relies on the “double clipping” of an orthogonal complex precursor. Such an approach was illustrated for Cu(I) templation in Figure 2, and an anion template analogue of this method was identified (Figure 17).<sup>25</sup> Thus, assembly of two of the acyclic precursors **27** followed by exposure to Grubbs’

catalyst in dichloromethane yields the doubly charged catenane **28**. Again, this approach is strongly dependent on the templating anion. Thus, for the precursor **27a–27b** complex, the two components arrange themselves around a single chloride anion, resulting in an exceptionally high yield of the [2]catenane product **28b** (78%). When the hexafluorophosphate salt **27b** was so treated, the [2]catenane product **28c** formed, but in much lower yield (16%). In this case, therefore, the secondary interactions alone are sufficient for the direct assembly of the orthogonal complex. However, the presence of a templating chloride anion substantially enhances the practicality of the reaction. When the chloride precursor **27a** was treated with Grubbs’ catalyst, the catenane product is also formed, in intermediate yield (34%). This is representative of a competition between the chloride template effect and the dominant 1:1 coordination stoichiometry of this system. Once again, the interlocked nature of the product may be demonstrated by spectroscopic and crystallographic means (Figure 18), which show the expected primary coordination of chloride and secondary hydrogen bonding and charge transfer interactions. Furthermore, it is possible to exchange the chloride anions of **28a** for hexafluorophosphate, thus removing the interweaving template.

This general anion templation methodology may therefore be used to prepare numerous interpenetrative assemblies which may then be clipped to form permanently interlocked catenane and rotaxane systems, in a manner

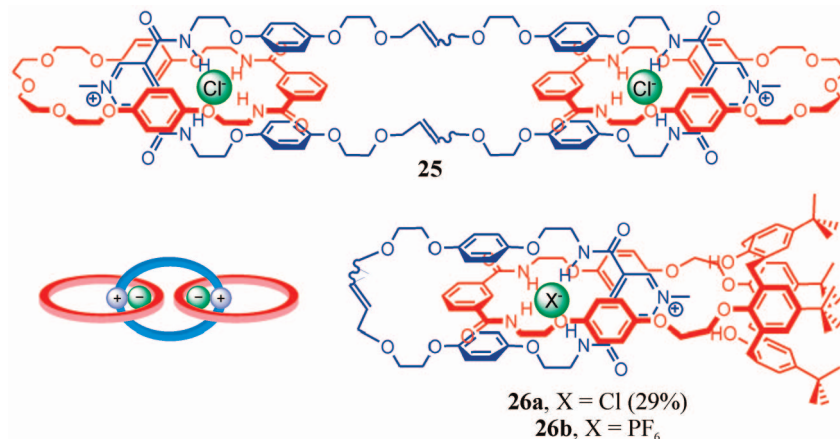


**FIGURE 16.** Alternative anion-templated catenanes: [3]catenane **25** (top and left) and calix[4]arene catenane **26** (bottom right).

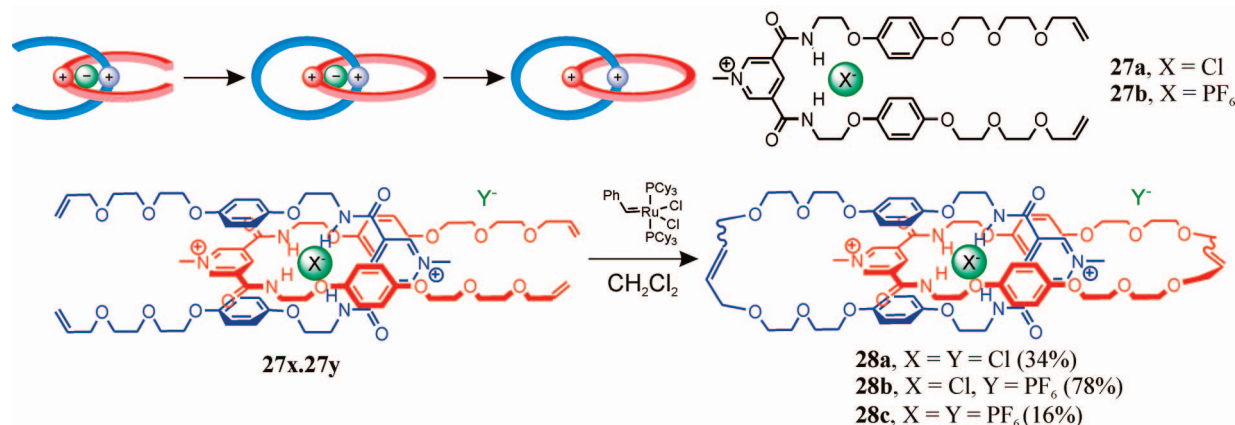


**FIGURE 17.** Double clipping route to [2]catenane. General schematic (top left), precursor molecule **27** (top right), and formation of [2]catenanes **28a–c** (bottom).

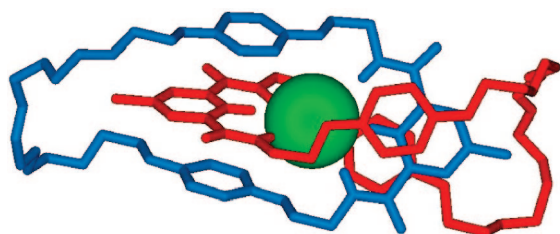


**FIGURE 18.** Single-crystal X-ray structure of **28b**. All hydrogens except those in the primary anion coordination sphere have been omitted for clarity. Chloride is represented as a space-filling sphere.

analogous to existing cation templation approaches. Importantly, these processes are critically dependent on the nature of the anion template but are highly tolerant of changes in assembly strategy and precursor structure. Furthermore, it is possible to remove the interweaving template in every case to furnish interlocked topologically unique binding domains. The properties of these domains form part of the discussion in the following section.

## Functional Properties of Anion-Templated Interlocked Systems

It was mentioned in the Introduction to this Account that a prime motivation for the investigation of such sophisticated architectures was the possibility for them to act in molecular-mechanical or device-like manners. The use

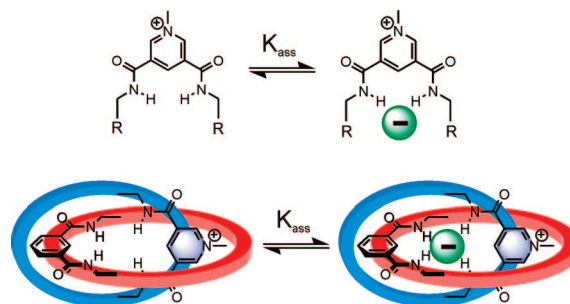


**FIGURE 19.** Anion binding by interlocked species. Two-dimensional hydrogen bonding by the parent pyridinium compound (top) and three-dimensional pocket provided by interlocked species such as a catenane (bottom).

of anion-templated interlocked derivatives for prototype sensory and mechanical materials was therefore investigated.

The removal of the halide anion templates from the interlocked architectures could be accomplished by treatment with silver hexafluorophosphate. This produced novel three-dimensional hydrogen bond-donating binding domains defined by the interpenetration of the two components, with the hexafluorophosphate anion too large to bind within it. The unique topology lends such anion-templated rotaxanes and catenanes potential unprecedented anion binding characteristics distinct from those of their “parent” species (Figure 19), as the non-interlocked components present linear convergent arrays



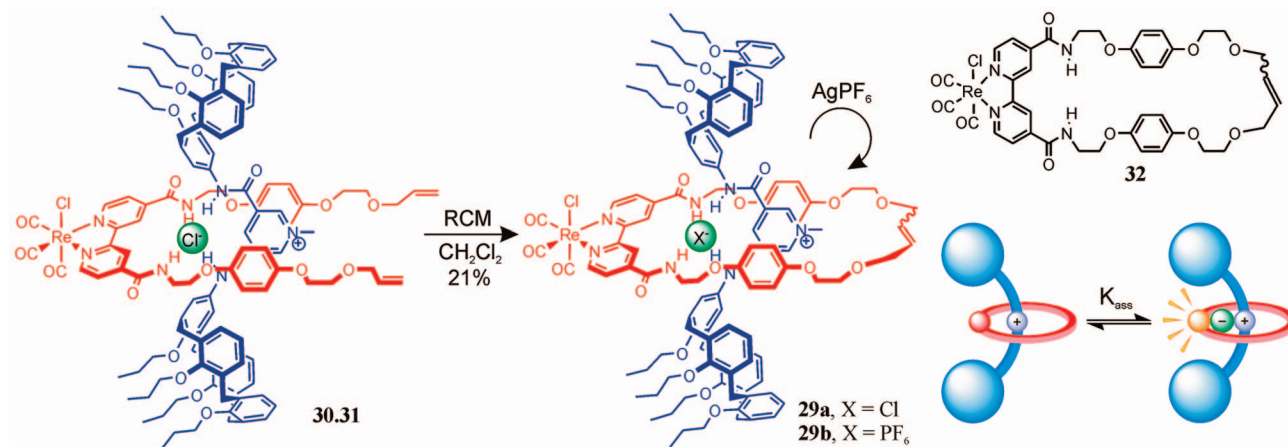


**FIGURE 20.** [2]Rotaxane anion sensor. Formation of rotaxanes **29a** and **29b** from precursors **30** and **31** by anion-templated Grubbs' ring closing metathesis (left), luminescent macrocycle **32** (top right), and schematic for rotaxane anion sensing (bottom right).

**Table 1.** Anion Binding Properties of Anion-Templated Rotaxanes and Catenanes and Their Asymmetric Pyridinium Precursors<sup>a</sup>

	thread	rotaxanes			thread	catenanes		
	<b>18d</b>	<b>19b</b>	<b>20b</b>	<b>21b</b>	<b>23d</b>	<b>24c</b>	<b>26b</b>	<b>28c</b>
Cl <sup>-</sup> ( $K_{11}$ )	125	<b>1130</b>	<b>4500</b>	<b>4500</b>	230	<b>730</b>	<b>960</b>	4320
H <sub>2</sub> PO <sub>4</sub> <sup>-</sup> ( $K_{11}$ )	260	300	1800	1500	1360	480	480	x <sup>c</sup>
H <sub>2</sub> PO <sub>4</sub> <sup>-</sup> ( $K_{12}$ )	— <sup>b</sup>	— <sup>b</sup>	180	— <sup>b</sup>	370	520	— <sup>b</sup>	x <sup>c</sup>
AcO <sup>-</sup> ( $K_{11}$ )	<b>22000</b>	100	930	725	<b>1500</b>	230	400	x <sup>c</sup>
AcO <sup>-</sup> ( $K_{12}$ )	140	40	— <sup>b</sup>	— <sup>b</sup>	345	— <sup>b</sup>	— <sup>b</sup>	x <sup>c</sup>

<sup>a</sup> Units of M<sup>-1</sup>, solvent of 1:1 CDCl<sub>3</sub>/CD<sub>3</sub>OD, errors of <10%. Values highlighted in bold correspond to the strongest 1:1 association constant for a given compound. <sup>b</sup> No 1:2 binding mode in the interaction with that anion. <sup>c</sup> Experiment not yet conducted. <sup>d</sup> Solvent, 1:1 acetone-*d*<sub>6</sub>/CDCl<sub>3</sub>.

of hydrogen bond donors. The anion binding properties of the rotaxane and catenane cavities were probed by <sup>1</sup>H NMR spectroscopic titration methods, largely in the 1:1 chloroform-*d*/methanol-*d*<sub>4</sub> solvent mixture, and are presented in Table 1.<sup>15,17,23–25</sup> It may clearly be seen from these data that the non-interlocked pyridinium precursor compounds preferentially bind the more basic anions dihydrogen phosphate and acetate; that is, they discriminate on the basis of charge density. The neutral macrocyclic components were not found to demonstrate significant anion binding in this solvent mixture. However, the interlocked rotaxanes and catenanes universally demonstrate selectivity for chloride, which is furthermore bound more strongly by these species than by the free acyclic pyridinium precursors. This increase in binding strength coupled with a reversal of selectivity is due to the provision of the encircled binding domain mentioned above, which allows good size, shape, and charge complementarity to the chloride anion, while precluding the binding of the more oxobasic acetate and dihydrogen phosphate on steric grounds. Thus, these architectures demonstrate anion binding properties dependent on the nature of the template used in their formation.

These results also indicate that it is possible to achieve the fine-tuning of the binding properties of the interlocked species by small changes in structure. Thus, among the rotaxanes, introduction of the electron-withdrawing nitro or iodo functionalities (**20b** or **21b**, respectively) leads to an enhancement in anion binding due to the increased acidity of the protons involved in hydrogen bond forma-

tion. Correspondingly, in the catenane systems, a doubling of the charge (**28c**) leads to a large increase in the chloride association constant. Given the general applicability of the templation methodology outlined in the previous section, it should be possible to prepare numerous other interlocked systems with superior anion binding selectivities, as well as for sensory purposes.

This potential was demonstrated by the formation and study of a luminescent [2]rotaxane system (Figure 20).<sup>26</sup> The chloride derivative **29a** was prepared in 21% yield through the now established ring clipping of the neutral rhenium(I) bipyridyl-containing precursor **30** around the pyridinium–chloride thread **31**; the bulky calix[4]arene stopper groups were necessary to prevent dethreading of the larger macrocycle. Again, replacement of the chloride template with hexafluorophosphate gave a [2]rotaxane **29b** which contained not only a three-dimensional anion binding domain but also a luminescent metal center which is capable of sensing the anion binding event. Thus, addition of TBA anion salts to a solution of **29b** in acetone induced an enhancement in the <sup>3</sup>MLCT emission band intensity of the receptor. Titration experiments in acetone demonstrated that the rotaxane selectively bound hydrogen sulfate ( $K_{\text{ass}} > 10^6 \text{ M}^{-1}$ ) over nitrate and chloride, which contrasts with the properties of the luminescent macrocycle **32**, which bound chloride selectively ( $K_{\text{ass}} = 8.7 \times 10^4 \text{ M}^{-1}$ ). An anion templation approach may therefore be used to generate molecular sensors for different anions, where the selectivity is based on the interlocked nature of the products.

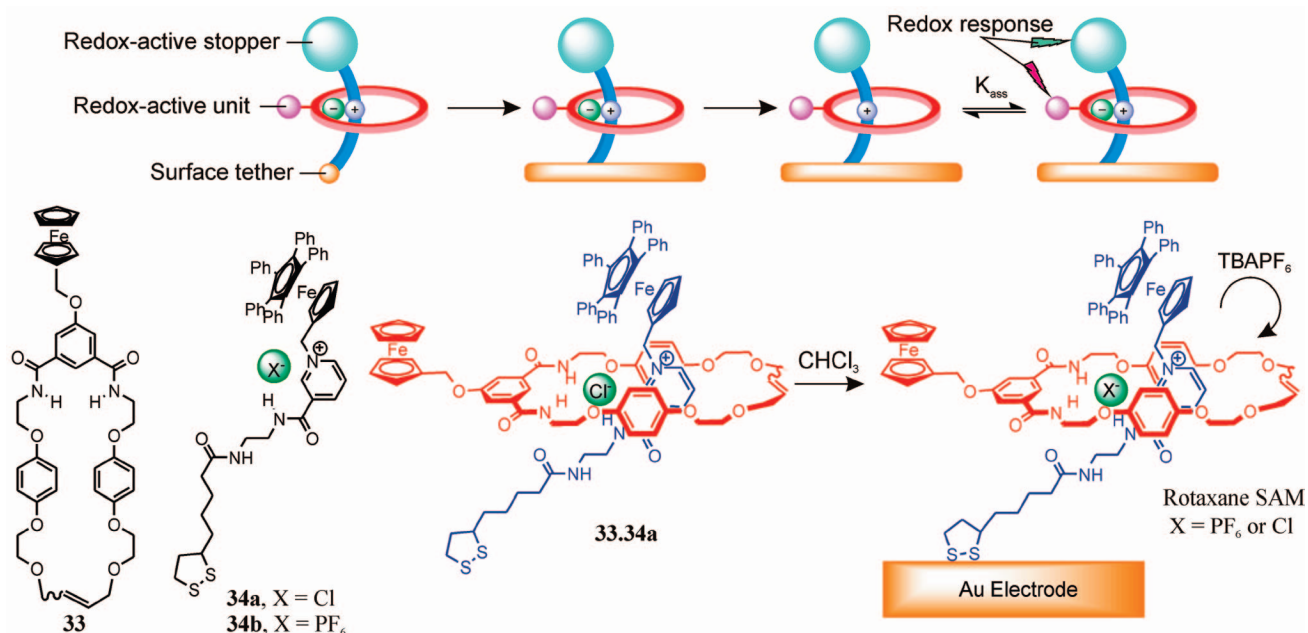


**FIGURE 21.** Anion-templated SAM rotaxanes for chloride sensing. General schematic (top), rotaxane SAM components (bottom left), and formation (bottom right).

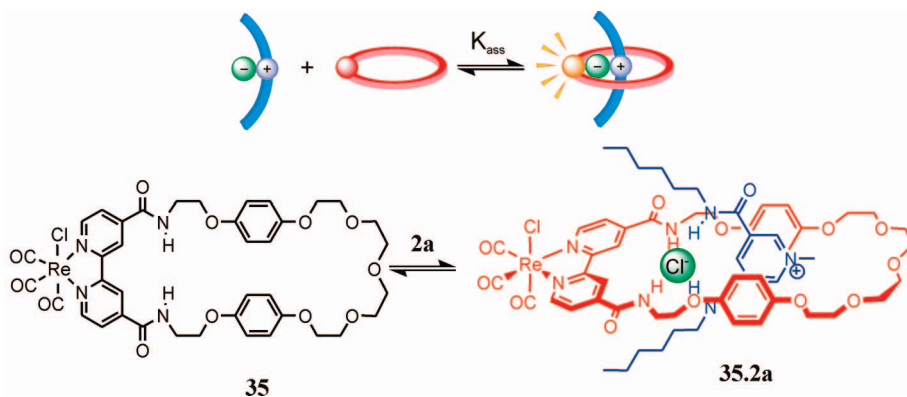


**FIGURE 22.** Luminescence sensing of [2]pseudorotaxane assembly using a rhenium-containing macrocycle. General schematic (top) and formation of pseudorotaxane **35.2a** (bottom).

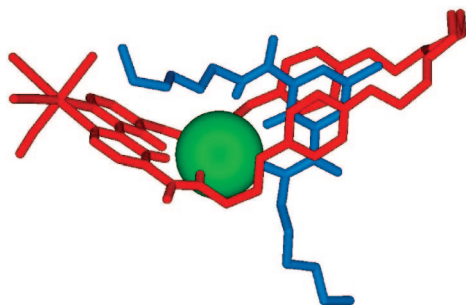


**FIGURE 23.** Single-crystal X-ray structure of **35.2a**. All hydrogens except those in the primary anion coordination sphere have been omitted for clarity. Chloride is represented as a space-filling sphere.

The confinement of such anion-templated systems at electrode surfaces should allow the harnessing of this specific binding behavior in electrochemical sensing materials. This possibility was probed by the formation of self-assembled monolayers (SAMs) of redox-active bis-ferrocene functionalized pseudorotaxane **33.34a** at a gold

surface; the transformation results in a rotaxane with the gold electrode effectively acting as one of the stoppers (Figure 21).<sup>27</sup> This assembly process was dependent on the presence of the chloride anion template as in previous systems, and again replacement of the chloride template with hexafluorophosphate proved to be possible without a disruption of the interlocked nature of the rotaxane SAM. The anion binding properties of this redox-active rotaxane SAM could be probed using electrochemical methods, examining the perturbations in the redox waves of the system's two ferrocene centers upon addition of a variety of analytes; proximal anion binding should be accompanied by a cathodic shift due to electrostatic stabilization of the oxidized ferrocene unit. In acetonitrile solutions, the ferrocene unit of the rotaxane macrocycle was shown to demonstrate a selective voltammetric response to chloride ( $\Delta E \sim 40$  mV), even in the presence of a 100-fold excess of competing anion such as dihydrogen phosphate. This contrasts sharply with the solution responses of the free thread **34b** and macrocycle **33**, which

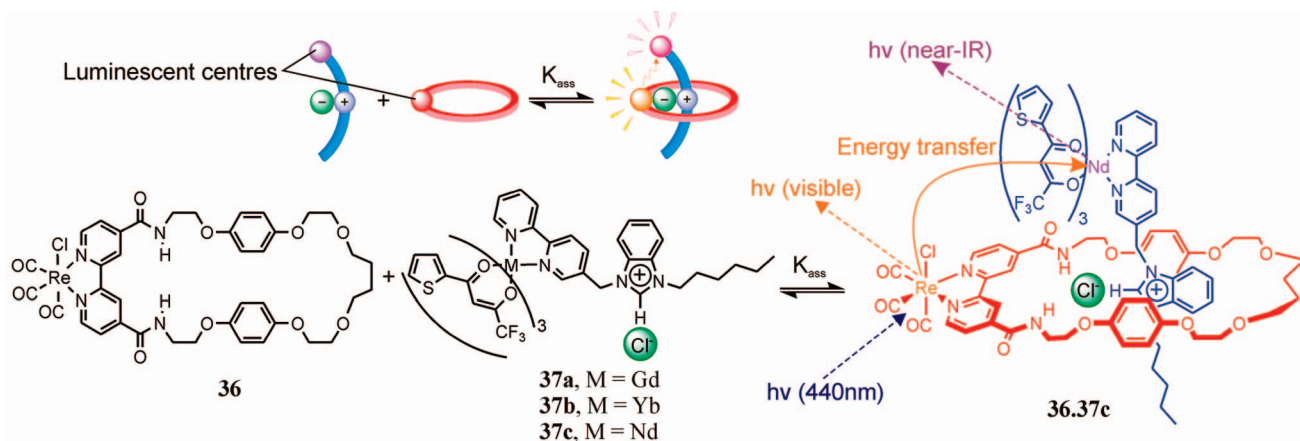


**FIGURE 24.** Sensing of [2]pseudorotaxane formation through Förster energy transfer. General schematic (top), luminescent macrocycle and thread components (bottom), and pseudorotaxane **36.37c** (right).

demonstrate small cathodic shifts in the presence of most anions, except for **33** with dihydrogen phosphate ( $\Delta E \sim 45$  mV) and hydrogen sulfate ( $\Delta E \sim 15$  mV). This therefore provides another example of the change in selectivity induced by the mutual interpenetration of two components, and further demonstrates the ability of this templation methodology to give sophisticated surface-confined species with very promising electrochemical recognition properties.

While the use of such permanently interlocked derivatives for sensing purposes demonstrates much promise, it would also be highly desirable to use this anion-templation phenomenon to direct and sense molecular movement. The threading of one component by another to form a [2]pseudorotaxane is a simple example of such movement, and methods of signaling this were therefore investigated. The first approach utilized the luminescent properties of rhenium(I) bipyridyl previously exploited for anion sensing (Figure 22).<sup>28</sup> The ability of the rhenium(I) bipyridyl motif to signal anion binding also allowed the detection of the anion-templated interpenetration of macrocycle **35** by a range of thread species, with an enhancement in the <sup>3</sup>MLCT luminescence emission band being observed upon addition of, for example, thread **2a** in acetone. <sup>1</sup>H NMR spectroscopic titration studies demonstrated that this enhancement corresponded to a threading process; these experiments were supported by the single-crystal X-ray structure of **35.2a** (Figure 23).

This molecular threading event may also be signaled using direct electronic communication between the thread and macrocycle components. The mechanism used to accomplish this was Förster energy transfer between a rhenium(I) bipyridyl center contained within macrocycle **36** and a lanthanide complex appended to the terminus of threads **37a–c** (Figure 24).<sup>29</sup> Addition of threads containing no lanthanide center, or a lanthanide center not suitable for energy transfer such as gadolinium (**37a**), to rhenium macrocycle **36** resulted in an enhancement of <sup>3</sup>MLCT luminescence emission, as observed in the case of **35.2a** described above. For threads containing a suitable lanthanide metal such as neodymium or ytterbium, however, no such enhancement was observed on pseudorotaxane formation;

indeed, for the neodymium thread **37b**, a significant quenching of rhenium-centered luminescence was observed. Furthermore, the evolution of new near-infrared emission bands consistent with lanthanide metal emission could be detected. This observation is consistent with the proposed Förster energy transfer between the <sup>3</sup>MLCT excited state of the rhenium(I) bipyridyl center and the lanthanide complex. As such an energy transfer process is highly dependent on the distance of separation between the two metal centers, the existence of such an interaction may be used to sense a direct interaction between the thread and macrocycle components, and hence pseudorotaxane formation.

To date, therefore, this general strategy for anion templation has been exploited in two main areas. The first concerns the removal of the anion template from permanently interlocked molecules, which gives receptors demonstrating binding properties dependent on the presence of a unique three-dimensional hydrogen bond-donating pocket, which is defined by the original anion template. By including optical and electrochemical readout functionalities and by attaching these derivatives to surfaces, we have begun to use such anion-templated structures for sensory purposes. Second, anion-templated molecular motion in the form of threading has been signaled by luminescence spectroscopic means. This opens the door for molecular machine-like devices based on anion recognition processes.

## Conclusion

A comprehensive anionic alternative to existing cation interweaving templation and self-assembly approaches has been devised and exploited in the assembly of numerous interpenetrated systems. These range from reversible assemblies such as orthogonal complexes and pseudorotaxanes to permanently interlocked derivatives such as rotaxanes and catenanes. Removal of the anion template from these permanently interlocked systems leads to novel receptor and sensory behaviors defined by the mutual interpenetration of the two components. This is distinct from many other literature interlocked systems stabilized by hydrogen bonding or charge transfer interactions which often lack such binding cavities, therefore negating the possibility of charged

guest recognition and sensing, and restricting machine-like responses to pH and redox control. The added synthetic versatility of anion templatation also allows for a much wider range of systems to be assembled which can be designed to exhibit a multiple choice of switchable chemical host-guest recognition-induced and/or electrochemical responses. These observations underline the general applicability and scope of this novel templatation strategy.

The anion templatation approach is, however, currently very much in its infancy; still only a handful of interlocked structures have been developed, and we are currently seeking to redress this balance, focusing on ever more complex motifs. The goal is ultimately to create increasingly sophisticated device-like structures to complement the impressive array of molecular machines already furnished through other templatation and self-assembly strategies. We also continue to be fascinated by the potential for these anion-templated architectures to be used for highly selective sensory devices for ionic substrates, and we aim to continue the development of such systems. As with the emergence of cationic interweaving templatation more than two decades ago, however, a huge catalogue of anion-templated structures has yet to be exploited.

*We thank the many workers and collaborators who have contributed significantly to the development of this templatation approach; their names appear in the appropriate references. We also acknowledge funding from the EPSRC, a Marie Curie Postdoctoral Fellowship of the European Union, the Natural Sciences and Engineering Research Council of Canada, GE Healthcare, the Clarendon Fund, and the Overseas Research Student (ORS) Awards Scheme.*

## References

- (1) Kay, E. R.; Leigh, D. A.; Zerbetto, F. Synthetic Molecular Motors and Mechanical Machines. *Angew. Chem., Int. Ed.* **2007**, *46*, 72–191.
- (2) Wasserman, E. The Preparation of Interlocking Rings: A Catenane. *J. Am. Chem. Soc.* **1960**, *82*, 4433–4434.
- (3) Harrison, I. T.; Harrison, S. Synthesis of a stable complex of a macrocycle and a threaded chain. *J. Am. Chem. Soc.* **1967**, *89*, 5723–5724.
- (4) Sauvage, J.-P.; Dietrich-Buchecker, C., Eds. *Molecular Catenanes, Rotaxanes and Knots: A Journey Through the World of Molecular Topology*; Wiley-VCH: Weinheim, Germany, 1999.
- (5) Ashton, P. R.; Glink, P. T.; Stoddart, J. F.; Tasker, P. A.; White, A. J. P.; Williams, D. J. Self-Assembling [2]- and [3]Rotaxanes from Secondary Dialkylammonium Salts and Crown Ethers. *Chem.—Eur. J.* **1996**, *2*, 729–736.
- (6) Anderson, S.; Anderson, H. L.; Sanders, J. K. M. Expanding Roles for Templates in Synthesis. *Acc. Chem. Res.* **1993**, *26*, 469–475.
- (7) Sauvage, J.-P. Interlacing molecular threads on transition metals: Catenands, catenates, and knots. *Acc. Chem. Res.* **1990**, *23*, 319–327.
- (8) Sessler, J. L.; Gale, P. A.; Cho, W.-S. *Anion Receptor Chemistry*; Royal Society of Chemistry: Cambridge, U.K., 2006.

- (9) Vilar, R. Anion-templated synthesis. *Angew. Chem., Int. Ed.* **2003**, *42*, 1461–1477.
- (10) Hübner, G. M.; Gläser, J.; Seel, C.; Vögtle, F. High-yielding rotaxane synthesis with an anion template. *Angew. Chem., Int. Ed.* **1999**, *38*, 383–386.
- (11) Schalley, C. A.; Silva, G.; Nising, C. F.; Linnartz, P. Analysis and improvement of an anion-templated rotaxane synthesis. *Helv. Chim. Acta* **2002**, *85*, 1578–1596.
- (12) Fyfe, M. C. T.; Hickingbottom, S. K.; Menzer, S.; Stoddart, J. F.; White, A. J. P.; Williams, D. J. Molecular meccano. 34. Combining different hydrogen-bonding motifs to self-assemble interwoven superstructures. *Chem.—Eur. J.* **1998**, *4*, 577–589.
- (13) Kavallieratos, K.; Bertao, C. M.; Crabtree, R. H. Hydrogen bonding in anion recognition: A family of versatile, nonpreorganized neutral and acyclic receptors. *J. Org. Chem.* **1999**, *64*, 1675–1683.
- (14) Wisner, J. A.; Beer, P. D.; Drew, M. G. B. A demonstration of anion templatation and selectivity in pseudorotaxane formation. *Angew. Chem., Int. Ed.* **2001**, *40*, 3606–3609.
- (15) Wisner, J. A.; Beer, P. D.; Drew, M. G. B.; Sambrook, M. R. Anion-Templated Rotaxane Formation. *J. Am. Chem. Soc.* **2002**, *124*, 12469–12476.
- (16) Sambrook, M. R.; Beer, P. D.; Wisner, J. A.; Paul, R. L.; Cowley, A. R.; Szemes, F.; Drew, M. G. B. Anion-Templated Assembly of Pseudorotaxanes: Importance of Anion Template, Strength of Ion-Pair Thread Association, and Macrocyclic Ring Size. *J. Am. Chem. Soc.* **2005**, *127*, 2292–2302.
- (17) Lankshear, M. D.; Evans, N. H.; Bayly, S. R.; Beer, P. D. Anion-Templated Calix[4]arene-Based Pseudorotaxanes and Catenanes. *Chem.—Eur. J.* **2007**, *13*, 3861–3870.
- (18) Wisner, J. A.; Beer, P. D.; Berry, N. G.; Tomapatanaget, B. Anion recognition as a method for templating pseudorotaxane formation. *Proc. Natl. Acad. Sci. U.S.A.* **2002**, *99*, 4983–4986.
- (19) Grubbs, R. H.; Miller, S. J.; Fu, G. C. Ring-Closing Metathesis and Related Processes in Organic Synthesis. *Acc. Chem. Res.* **1995**, *28*, 446–452.
- (20) Mohr, B.; Sauvage, J.-P.; Grubbs, R. H.; Weck, M. High-Yield Synthesis of [2]Catenanes by Intramolecular Ring-Closing Metathesis. *Angew. Chem., Int. Ed.* **1997**, *36*, 1308–1310.
- (21) Frey, J.; Kraus, T.; Heitz, V.; Sauvage, J.-P. A catenane consisting of a large ring threaded through both cyclic units of a handcuff-like compound. *Chem. Commun.* **2005**, 5310–5312.
- (22) Wakabayashi, R.; Kubo, Y.; Kaneko, K.; Takeuchi, M.; Shinkai, S. Olefin Metathesis of the Aligned Assemblies of Conjugated Polymers Constructed through Supramolecular Bundling. *J. Am. Chem. Soc.* **2006**, *128*, 8744–8745.
- (23) Sambrook, M. R.; Beer, P. D.; Lankshear, M. D.; Ludlow, R. F.; Wisner, J. A. Anion-templated assembly of [2]rotaxanes. *Org. Biol. Chem.* **2006**, *4*, 1529–1538.
- (24) Sambrook, M. R.; Beer, P. D.; Wisner, J. A.; Paul, R. L.; Cowley, A. R. Anion-Templated Assembly of a [2]Catenane. *J. Am. Chem. Soc.* **2004**, *126*, 15364–15365.
- (25) Ng, K.-Y.; Cowley, A. R.; Beer, P. D. Anion templated double cyclization assembly of a chloride selective [2]catenane. *Chem. Commun.* **2006**, 3676–3678.
- (26) Curiel, D.; Beer, P. D. Anion directed synthesis of a hydrogensulfate selective luminescent rotaxane. *Chem. Commun.* **2005**, 1909–1911.
- (27) Bayly, S. R.; Gray, T. M.; Chmielewski, M. J.; Davis, J. J.; Beer, P. D. Anion templated surface assembly of a redox-active sensory rotaxane. *Chem. Commun.* **2007**, in press.
- (28) Curiel, D.; Beer, P. D.; Paul, R. L.; Cowley, A. R.; Sambrook, M. R.; Szemes, F. Halide anion directed assembly of luminescent pseudorotaxanes. *Chem. Commun.* **2004**, 1162–1163.
- (29) Sambrook, M. R.; Curiel, D.; Hayes, E. J.; Beer, P. D.; Pope, S. J.; Faulkner, S. Sensitized near infrared emission from lanthanides via anion-templated assembly of d-f heteronuclear [2]pseudorotaxanes. *New J. Chem.* **2006**, *30*, 1133–1136.

AR7000217